Continuous Space-Time Crystal State Driven by Nonreciprocal Optical Forces

V. Raskatla[1], T. Liu[1], J. Li[2], K. F. MacDonald[1], and Nikolay I. Zheludev[1, 2]

[1] *Optoelectronics Research Centre, University of Southampton, Highfield, Southampton, SO17 1BJ, UK*

[2] *Centre for Disruptive Photonic Technologies & The Photonics Institute, SPMS, Nanyang Technological University, Singapore 637371*

We show that the continuous time crystal state can arise in an ensemble of linear oscillators from nonconservative coupling via optical radiation pressure forces. This new mechanism comprehensively explains observations of the time crystal state in an array of nanowires illuminated with light [Nat. Phys. 19, 986 (2023)]. Being fundamentally different from regimes of nonlinear synchronization, it has relevance to a wide range of interacting many-body systems including in the realms of chemistry, biology, weather, and nanoscale matter.

Time crystals – a state of matter with spontaneously broken time-translation symmetry, were introduced theoretically just over a decade ago [1-4]. It was subsequently understood that nature prohibits the breaking of continuous time translation symmetry in closed systems [5]. However, time crystals with broken discrete time-translation symmetry, wherein an external periodic force initiates spontaneous oscillation at sub-harmonic frequency, have been experimentally realized in a variety of trapped ion and atom, solid state spin, and superconducting qubit systems [4]. Open systems that break continuous time translation symmetry realize the spirit of the original proposal more closely and represent a new state of matter. A continuous time crystal is a many-body system in which continuous time translation symmetry is spontaneously broken into periodic motion in response to an arbitrarily weak perturbation via a first-order, ergodicity-breaking phase transition (distinguishing it from classical oscillation phenomena). Such behavior has been seen in the slow oscillation dynamics of a semiconductor nonlinear electron-nuclear spin system at few-Kelvin temperatures [6]; in a strongly interacting Rydberg gas at room temperature [7]; and in an optically pumped dissipative Bose-Einstein condensate in an optical cavity [8]. In the latter, time-periodic light emission and spatially periodic atomic density emerge spontaneously, and the system therefore constitutes a continuous *space-time* crystal.

These observations in quantum atomic and spin systems demonstrate the feasibility of the continuous (space-)time crystal state but do not provide "materials" suitable for practical applications. However, it has recently been shown experimentally that a simpler classical system – an array of dielectric nanowires decorated with plasmonic metamolecules (a metamaterial) undergoing stochastic thermal motion, can be optically driven into a state of robust, persistent, coherently synchronized oscillation [9]. Despite its physical periodicity, this array lacks spatial periodicity as the nanowires exhibit uncorrelated in- and out-of-plane thermal motion. Upon synchronization, they exhibit phase-locked, amplified out-of-plane motion, spontaneously breaking continuous spatial and temporal translational symmetry. As such, the system becomes a classical (as opposed to quantum, c.f. Refs. [1, 2]) continuous space-time crystal (CSTC) material, potentially deployable in electrooptic, timing and sensing applications.

We show here that this transition to the CSTC state belongs to a class of phase transitions driven by non-reciprocal forces [10, 11]. Nonreciprocal interactions in many-body systems are increasingly understood to underpin a multifarious range of emergent phenomena across physical and bio sciences [12-17]: For example, colloidal particles and enzymes exhibit non-reciprocal interactions when they are catalytically active; 'chasing' interactions between non-polar particles in a binary mixture lead to the emergence of polarity in the form self-organized self-propelled active molecules, and among more than two species can introduce time-periodic clustering; nonreciprocal interactions can lead to novel phase transitions, self-organization, formation of complex spatiotemporal patterns accompanied by parity and time-reversal symmetry breaking, space- and time-translation symmetry breaking, and spontaneous chiral symmetry breaking.. Of particular relevance to the present case, it has been shown theoretically, and in simple robotic demonstrations, that nonreciprocal interactions can lead to synchronization [11, 14, 15], which can be described in the framework of bifurcation theory and non-Hermitian quantum mechanics.

We demonstrate here that light can be the agent of nonreciprocity in such transitions, leading to synchronization of oscillator movements, the establishment of spatial periodicity, and breaking of ergodicity in the transition to the CSTC state. Optical forces are generally perceived to be conservative and reciprocal, e.g. optical trap forces proportional to the light intensity gradient. However, in a non-Hamiltonian ensemble of oscillators, in the presence of light which continuously pumps energy into the system, nonreciprocal forces can emerge from the radiation pressure induced by scattered fields [18-25]. (Note here that 'nonreciprocal' refers to breaking of the action-reaction equality, rather than the reciprocity of

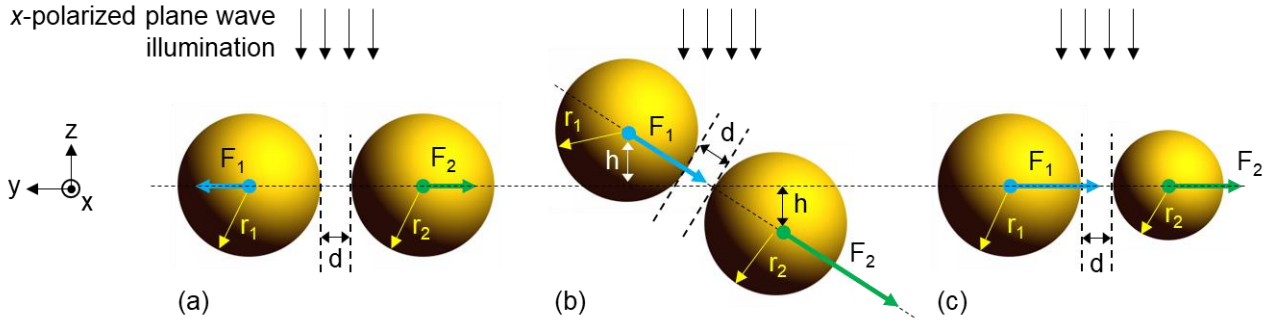

Fig. 1. Light-induced nonreciprocal optical forces. Optical forces $\boldsymbol{F_1}$, $\boldsymbol{F_2}$ acting on a pair of spherical gold nanoparticles along their centre-to-centre axis under illumination with *x*-polarized light at a wavelength of 550 nm at an intensity of 1327 μW/μm^2 when the particles are: (a) of the same size and illuminated in phase; (b) of the same size and illuminated with a relative phase lag; **(c)** of different sizes. The specific values of parameters are as follows: (a) r_1, r_2 = 60 nm, d = 40 nm, $\boldsymbol{F_1} = -\boldsymbol{F_2}$ = -1.5 fN, (b) r_1, r_2 = 60 nm, d = 40 nm, h = 40 nm, $\boldsymbol{F_1}$ = 30 fN, $\boldsymbol{F_2}$ = 64 fN, (c) r_1 = 60nm, r_2 = 40 nm, d = 40 nm, $\boldsymbol{F_1}$ = 9 fN, $\boldsymbol{F_2}$ = 5 fN.

electromagnetic field propagation introduced through the Lorentz and Feld-Tai lemmas [26, 27].) The nonconservative component can be significant in nanoscale systems, leading to apparent violations of the action-reaction equality, as illustrated in Fig. 1 for the simple case of two closely spaced plasmonic nanoparticles under continuous plane wave coherent illumination. When the particles are of the same size and aligned with their center-to-center axis parallel to the incident wavefront (Fig. 1a), light-induced forces acting on the particles along that axis are reciprocal ($\boldsymbol{F1 = -F2}$). However, if they are illuminated with a mutual phase lag (Fig. 1b) or differ in size/shape (Fig. 1c), the forces along the shared axis are generally neither of equal magnitude nor opposite sign.

Now consider a simplified model of the CSTC demonstrated in Ref. [9] - a 2D array of nanowires decorated with plasmonic nanorods. We will examine two cases: one in which all nanowires are identical (all decorated with the same type of plasmonic particles, Fig. 2a); and another in which there are two alternating types of nanowire decorated with different nanoparticles (Fig 2b). We assume that in the presence of light, identical nanowires interact reciprocally, while differing nanowires interact nonreciprocally, and begin by analyzing the motion of isolated nanowire pairs. Their thermal motion at non-zero temperatures is accounted for by assuming that they are connected to a common bath (the metamaterial frame) at temperature T. Such a system is described by the Langevin model for linear oscillators,

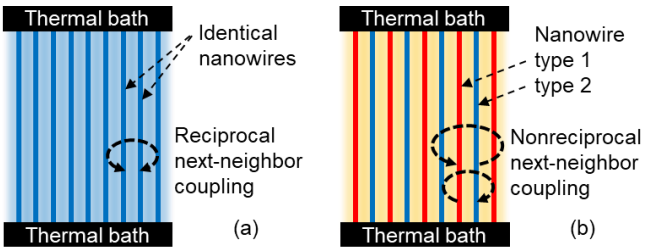

Fig. 2. Schematics of nanowire metamaterials, in which: (a) all nanowires are identical and thereby reciprocally coupled in the presence of light; (b) alternate nanowires support different nanoparticles, such that they can be nonreciprocally coupled when illuminated.

with frequencies ω_{0i}, masses m_i and loss parameters $\gamma_i = \omega_{0i}/Q_i$:

$$\ddot{x}_i + \gamma_i \dot{x}_i + \omega_{0i}^2 x_i + \sum \xi_{ij}\left(x_i - x_j\right) = \sqrt{2k_B T \gamma_i / m_i}\,\eta_i(t) \qquad (1)$$

where Q_i and $\eta_i(t)$ are respectively quality factors and normalized white noise terms, and the parameter ξ_{ij} describes light-induced coupling between oscillators.

We analyze the behavior of these systems under various coupling conditions by numerically solving the stochastic differential Eq. (1) (using Heun's method [28]; see Supplementary Material), taking values of ω_{0i}, m_i, γ_i close to those of the Ref. [9] experimental system. From Maxwell tensor calculations, electromagnetic forces acting between nanoparticles in the experimental case are found to be predominantly nonreciprocal (see Supplementary Material). However, to illustrate differences between reciprocal $\xi_{12} = \xi_{21} = \xi$ and nonreciprocal $\xi_{12} = -\xi_{21} = \xi^*$ coupling we consider both cases.

We first consider identical oscillators ($\omega_{01} = \omega_{02} = \omega_0$; $\gamma_1 = \gamma_2$). Figure 3a shows spectra of oscillator positions $x_1(t)$ and $x_2(t)$ in the absence of coupling, calculated from 1 ms intervals of time-series data (~2000 oscillation cycles): they identically exhibit resonances at the oscillators' fundamental frequency ω_0. When reciprocal coupling is introduced, the resonances split: for each oscillator, one peak remains at ω_0, while a 'run-away' resonance at $\tilde{\omega}_0$ appears and either increasingly blue- or red-shifts (relative to ω_0) with increasing coupling strength ξ. While the two oscillators' motion spectra are the same in the presence of reciprocal coupling, their movement is uncorrelated regardless to the value of ξ. This can be seen from the persistently random variation of the order parameter $r(t) = \frac{1}{2} abs\left\{e^{i\varphi_1(t)} + e^{i\varphi_2(t)}\right\}$ as a function of time (Fig. 3d) – this being a measure of synchrony: a stable value of r means that the phase lag $\varphi_1(t) - \varphi_2(t)$ between oscillations is constant and they are synchronized; $r = 1$ corresponds to the oscillators moving in phase.

In the case of nonreciprocal coupling ($\xi_{12} = -\xi_{21} = \xi^*$), oscillator dynamics are radically different: firstly, there is no resonance splitting (Fig. 3c – here, we no

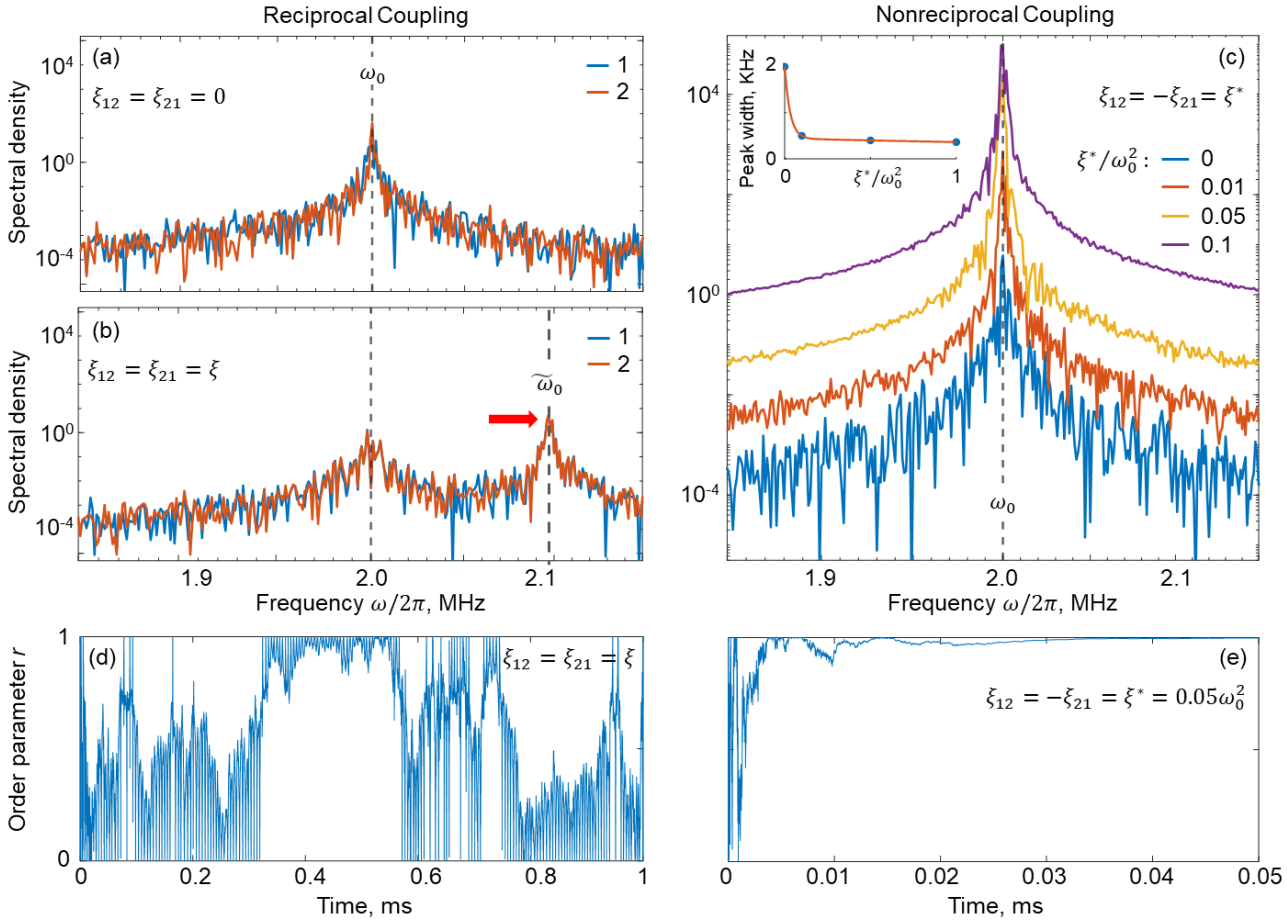

Fig. 3. Dynamics of coupled noisy, identical, linear oscillators. (a, b) Spectral density of position for a pair of identical noise-driven oscillators [1 and 2] with natural frequency $\omega_0/2\pi = 2$ MHz, effective mass 1 pg and quality factor $Q = 1000$, at $T = 300$K in the case of: (a) no coupling between oscillators: $\xi_{12} = \xi_{21} = 0$; (b) reciprocal coupling:$\xi_{12} = \xi_{21} = \xi = 0.05\omega_0^2$; (c) Spectral density of position for one of two identical nonreciprocally coupled oscillators, for a selection of coupling strengths ξ^* [as labelled]. The inset shows resonance width as a function of ξ^*. (d, e) Order parameter as a function of time for: (d) the reciprocally coupled system, from the moment in time when coupling reaches $\xi = 0.05\omega_0^2$; (e) nonreciprocal coupling from $\xi^* = 0.05\omega_0^2$ [the yellow trace in panel (c)].

longer plot separate spectra for the two oscillators, but rather just one of them). Instead, oscillation amplitude grows with increasing ξ^*, and the resonance narrows (see inset to Fig. 3c). Moreover, relative noise decreases, and the synchronized oscillation resembles that of a single oscillator with amplitude and quality factor growing with ξ^* (Fig 3c). The oscillators' movements become correlated, more quickly with stronger nonreciprocal coupling. After an initial transition period, the order parameter asymptotically approaches $r = 1$, as shown in Fig. 3e.

Next, we consider synchronization due to nonreciprocal coupling between two oscillators with different natural frequencies, $\omega_{01} = \omega_0 - \delta\omega$ and $\omega_{02} = \omega_0 + \delta\omega$, where $\gamma \ll \delta\omega \ll \omega_0$. This is a case of particular practical importance because manufacturing tolerances in real time-space metamaterials inevitably lead to variations among nanowires' fundamental oscillation frequencies.

For reciprocally coupled identical oscillators the run-away resonance splits (by ξ/ω_0) from their shared natural frequency, as shown in Fig. 3b. More generally, when the oscillators' (uncoupled) natural frequencies are different, both resonances shift in the same direction (depending on the sign of ξ) with increasing coupling strength; one tends to ω_0 while the other keeps running. This is a manifestation of anti- (or avoided) crossing [29], arising due to the additional restoring force caused by reciprocal interaction, increasing the oscillation frequency.

Synchronization of non-identical oscillators is achievable when coupling is nonreciprocal, but only above a threshold coupling strength ξ^*_{th}. Figure 4a shows the spectral density of relative position for a pair of dissimilar oscillators for various values of ξ^*. In the absence of coupling (blue line), two peaks are seen at the oscillators' fundamental frequencies. As ξ^* approaches ξ^*_{th}, the peaks shift towards one another and collapse into a single resonance at ω_0 (orange line). Further increasing the coupling strength leads to an exponential, orders-of-magnitude increase in oscillation amplitude and a decrease in relative noise (yellow line). Synchronization is also manifested in the order parameter, which evolves rapidly (as a function of increasing coupling strength, Fig. 4b) to a stable value corresponding to a stable phase difference between the oscillators (which is a function of $\delta\omega$).

It should be noted here that the amplitude of synchronized oscillation (above the ξ^*_{th} threshold) grows with time. Spectra are therefore calculated from short (1

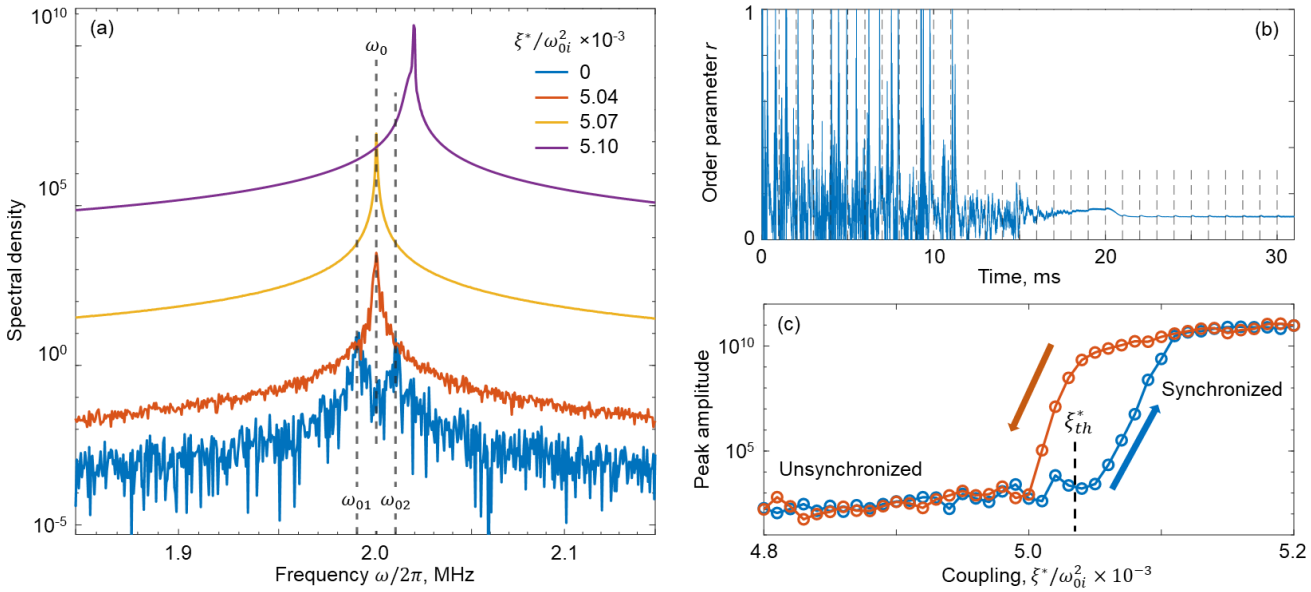

Fig. 4. Dynamics of nonreciprocally coupled noisy, non-identical oscillators. (a) Spectral density of relative position for a pair of nonreciprocally coupled oscillators at various coupling strengths. Here, the presence of nonlinearity is manifested by frequency pulling at high coupling strength (the purple curve). The vertical dashed lines indicate the individual fundamental and mean oscillation frequencies. (b) Order parameter as a function of time, where coupling strength increases from zero at time = 0, in increments of $0.00001\omega_{0i}^2$ at 1 ms intervals (denoted by the dashed lines). (c) Peak amplitude of spectral density as a function of increasing (blue) and decreasing (orange) coupling strength. The vertical dashed line indicates the coupling threshold, ξ^*_{th} for onset of synchronization.

ms; ~2000 period) intervals of $x_{1,2}(t)$ data, during which oscillation amplitude grows by only a few percent. In real systems, increasing amplitude is constrained by nonlinearity – in the case of doubly-clamped nanowires, by their mechanical or 'geometric' nonlinearity: when displacement amplitude is comparable to the thickness of the nanowire, the nonlinear component of restoring force becomes comparable to the linear 'Hooke's law' force [30]. To account for this in modelling, we add a cubic nonlinearity term $10^9\omega_{0i}^2x_i^3$ to the left-hand side of Eq. 1, which has the effect of limiting the (otherwise exponential) growth of oscillation amplitude at the level comparable to the nanowire thickness in experiments. It also pushes the synchronized oscillation frequency away from ω_0 towards higher frequencies (as shown by the purple line in Fig. 4a). The saturation of oscillation amplitude as a function of increasing coupling strength is shown in Fig. 4c, which also reveals a hysteresis in synchronization – an important characteristic of a first-order phase transition.

It must be emphasized here that the oscillators' nonlinearity is not required for their synchronization, as it would be in other regimes (e.g. Kuramoto) that depend on nonlinearity [31]: it only manifests itself at large (already synchronized) amplitudes, as effectively a limiting mechanism.

Finally, we illustrate the synchronization process for an array of six inhomogeneously broadened oscillators, each nonreciprocally coupled to their nearest neighbors. This demonstrates one of the most characteristic features of the CSTC regime – loss of ergodicity. We employ the same equations as above (with indices i, j taking values from 1 to 6). We assume $\xi_{ij}/\omega_{0i}^2 = -\xi_{ji}/\omega_{0j}^2 = X \times 10^{-3}$ for all values of i, j, and that oscillators are coupled to near neighbors only. (There is no coupling between the first and the last oscillators in the array.) We assume frequencies $\omega_{0,1-6}/2\pi = 1.961,\ 2.025,\ 1.979,\ 2.010,\ 1.974,\ 2.023$ MHz and include the abovementioned cubic nonlinearity term $10^9\omega_{0i}^2x_i^3$.

At low coupling strengths, the phase space of the system is rich, the oscillators move stochastically, and spectra contain six separate peaks at different frequencies, as shown at the bottom of Fig. 5 (where $X = 4.0$). With increasing coupling (Fig. 5a), some of the resonances merge and then demerge, temporarily creating 'domains' of neighboring oscillators that move in unison (e.g. $i = 3,4$ at $X = 4.25$). At $X = 4.65$ oscillators $i = 2,3,4,5$ become robustly synchronized and then at $X_{th}^{cryst} = 4.7$ they are joined by the remaining oscillators $i = 1,6$. Synchronization is complete and ergodicity of the system has been broken: the ensemble's phase space has collapsed into a single unified trajectory. With decreasing,

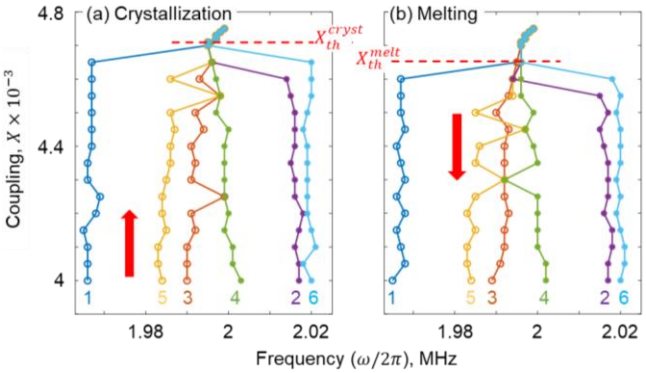

Fig. 5. Crystallization and melting of a space-time crystal. Synchronization (crystallization) and de-synchronization (melting) in an ensemble of six nonreciprocally coupled oscillators. The numerical annotations at the bottom of each line denote the position of the oscillator within the array.

coupling the synchronized state breaks at $X_{th}^{cryst} < X_{th}^{melt}$ (hysteresis). The restoration of stochastic motion also goes through stages of disintegration and domain formation, as can be seen in Fig. 5b.

In conclusion, we have demonstrated that the recent observation of a light-induced continuous space-time crystal state in a metamaterial array of interacting nanowires decorated with plasmonic nanoparticles can be comprehensively explained as a nonreciprocal phase transition, occasioning spontaneous synchronization, establishment of spatial periodicity, and loss of motion ergodicity. The findings offer insight to the understanding of a diverse range of systems involving nonreciprocal interactions [10-17].

This work was supported by the UK Engineering and Physical Sciences Research Council (grant EP/T02643X/1 – NIZ, KFM) and the National Research Foundation Singapore (grant NRF-CRP23-2019-0006 - NIZ).

Data availability: All necessary information to reproduce the results presented is contained within the article and the Supplementary Material. A representative set of oscillator positional time-series data for this paper can also be obtained from the University of Southampton ePrints research repository: https://doi.org/10.5258/SOTON/D3200.

[1] F. Wilczek, Phys. Rev. Lett. **109**, 160401 (2012).

[2] A. Shapere, and F. Wilczek, Phys. Rev. Lett. **109**, 160402 (2012).

[3] K. Sacha, *Time Crystals* (Springer Nature, Switzerland, 2020).

[4] M. P. Zaletel, M. Lukin, C. Monroe, C. Nayak, F. Wilczek, and N. Y. Yao, Rev. Mod. Phys. **95**, 031001 (2023).

[5] H. Watanabe, and M. Oshikawa, Phys. Rev. Lett. **114**, 251603 (2015).

[6] A. Greilich, N. E. Kopteva, A. N. Kamenskii, P. S. Sokolov, V. L. Korenev, and M. Bayer, Nat. Phys. **20**, 631 (2024).

[7] X. Wu, Z. Wang, F. Yang, R. Gao, C. Liang, M. K. Tey, X. Li, T. Pohl, and L. You, Nat. Phys. (2024).

[8] P. Kongkhambut, J. Skulte, L. Mathey, J. G. Cosme, A. Hemmerich, and H. Kessler, Science **377**, 670 (2022).

[9] T. Liu, J. Y. Ou, K. F. MacDonald, and N. I. Zheludev, Nat. Phys. **19**, 986 (2023).

[10] N. P. Kryuchkov, A. V. Ivlev, and S. O. Yurchenko, Soft Matter **14**, 9720 (2018).

[11] M. Fruchart, R. Hanai, P. B. Littlewood, and V. Vitelli, Nature **592**, 363 (2021).

[12] C. H. Meredith, P. G. Moerman, J. Groenewold, Y.-J. Chiu, W. K. Kegel, A. van Blaaderen, and L. D. Zarzar, Nat. Chem. **12**, 1136 (2020).

[13] R. Soto, and R. Golestanian, Phys. Rev. Lett. **112**, 068301 (2014).

[14] Z. You, A. Baskaran, and M. C. Marchetti, Proc. Natl. Acad. Sci. **117**, 19767 (2020).

[15] N. Uchida, and R. Golestanian, Phys. Rev. Lett. **104**, 178103 (2010).

[16] A. Sengupta, T. Kruppa, and H. Löwen, Phys. Rev. E **83**, 031914 (2011).

[17] D. S. Calovi, U. Lopez, S. Ngo, C. Sire, H. Chaté, and G. Theraulaz, New. J. Phys. **16**, 015026 (2014).

[18] S. Sukhov, A. Shalin, D. Haefner, and A. Dogariu, Opt. Express **23**, 247 (2015).

[19] Y. Arita, S. H. Simpson, P. Zemánek, and K. Dholakia, Sci. Adv. **6**, eaaz9858 (2020).

[20] H. G. Craighead, Science **290**, 1532 (2000).

[21] M. Reisenbauer, H. Rudolph, L. Egyed, K. Hornberger, A. V. Zasedatelev, M. Abuzarli, B. A. Stickler, and U. Delić, arXiv:2310.02610v2 (2023).

[22] R. Zhao, P. Tassin, T. Koschny, and C. M. Soukoulis, Opt. Express **18**, 25665 (2010).

[23] H. Rudolph, U. Delić, K. Hornberger, and B. A. Stickler, arXiv:2306.11893 (2023).

[24] J. Rieser, M. A. Ciampini, H. Rudolph, N. Kiesel, K. Hornberger, B. A. Stickler, M. Aspelmeyer, and U. Delić, Science **377**, 987 (2022).

[25] M. Antognozzi, C. R. Bermingham, R. L. Harniman, S. Simpson, J. Senior, R. Hayward, H. Hoerber, M. R. Dennis, A. Y. Bekshaev, K. Y. Bliokh, and F. Nori, Nat. Phys. **12**, 731 (2016).

[26] C. T. Tai, IEEE T. Antenn. Propag. **40**, 675 (1992).

[27] W. C. Chew, IEEE T. Antenn. Propag. **56**, 970 (2008).

[28] K. Burrage, I. Lenane, and G. Lythe, SIAM J. Sci. Comput. **29**, 245 (2007).

[29] K. K. Likharev, "Essential Graduate Physics - Classical Mechanics," (LibreTexts Physics).

[30] D. Papas, J. Y. Ou, E. Plum, and N. I. Zheludev, Adv. Sci. **10**, 2300042 (2023).

[31] A. Pikovsky, M. Rosenblum, and J. Kurths, *Synchronization: A Universal Concept in Nonlinear Sciences* (Cambridge University Press, Cambridge, 2001).